IEEE 802.11p for Vehicle-to-Vehicle (V2V) Communications

Zijun Zhao and Xiang Cheng
School of Electronics Engineering and Computer Science, Peking University, Beijing, China.
Email: {zhaozijun, xiangcheng}@pku.edu.cn

***Abstract*—This report focuses on the channel estimation problem in IEEE 802.11p based vehicle-to-vehicle (V2V) communications, which is very challenging in view of the extremely time-varying characteristics of mobile channels. Specifically, we propose a novel channel estimator named constructed data pilot (CDP) estimator for the current communication standards, by fully exploiting the channel correlation characteristics across two concatenated symbols. On the basis of the CDP estimator, we further resort to two efficient techniques to improve its performance over the entire signal-to-noise ratio (SNR) region. For the first technique, the time-variant mobile channel is modeled as a first-order Markov process so that the exact autocorrelation value of the two adjacent symbols can be derived. For the second technique, the SNR is estimated and serves as a priori information. Simulation results reveal that our proposed channel estimators outperform existing alternatives with lower computational complexity.**

***Index Terms*—Orthogonal frequency division multiplexing (OFDM), IEEE 802.11p, vehicle-to-vehicle (V2V) communications, channel estimation, constructed data pilot (CDP).**

I. Introduction

In the recent years, traffic accidents have become one of the leading causes for death all over the world, hence road safety has been greatly concerned. At the same time, we are facing the pressing needs for convenience and commercial oriented applications onboard. Vehicle-to-vehicle (V2V) communication, as a promising technique of intelligent transportation system, has been proposed to meet these needs. Over the past decade, V2V communications have attracted a lot of attention and various applications have been developed, such as the cooperative forward collision warning, traffic light optimal speed advisory, remote wireless diagnosis [1], etc. In 2010, after a few years test run, IEEE 802.11p standard, which is also referred to as dedicated short range communications standard [2], has been officially implemented.

Channel estimation technique plays an important role for the design of any communication systems. As far as we know, a precisely estimated channel response (CR) is critical for the follow-up equalization, demodulation, and decoding. Therefore, generally speaking, the accuracy of the channel estimation decides system performance. However, According to [3], the maximum Doppler frequency in V2V communications can be four times higher than that in cellular scenarios with the same velocity. As a consequence, the time-varying characteristics of vehicular environments are extremely prominent which make the channel estimation very challenging.

For V2V communication systems, the design of channel estimation technique is much more difficult and significant than any other wireless systems. However, the IEEE 802.11p is originally derived from the well-known standard IEEE 802.11a, which was initially designed for relatively stationary indoor environments, without considering the impact of high mobility. This results in the current IEEE 802.11p standard having several deficiencies to properly suit high dynamic property of V2V channels. This report focuses on one of the most important challenge among these deficiencies: how to properly design the channel estimation module for IEEE 802.11p standard. In general, there are two basic manners. The first one needs the modification of the structure of the IEEE 802.11p [4]–[10], while the other one adheres to the structure of the IEEE 802.11p standard [11]–[23].

First of all, the channel estimation schemes belonged to the first manner are briefly described. In [4], a midamble assisted scheme was first proposed and further investigated in [5] and [6]. Considering that the traditional preamble ahead of data cannot support reliable channel updating, midamble sequences are periodically inserted between data symbols to enable continuous channel information tracking. In [7]–[9], pseudo-random sequences are also inserted into guard intervals (GIs) to improve estimation performance, which was originated from [10].

Evidently, modifying the standard frame structure is a shortcut to obtain satisfactory performance improvement as well as simplifying the estimation. However, the compatibility with other standard IEEE 802.11p receivers is severely impaired. Therefore, the majority of the current channel estimation schemes adopt the aforementioned second approach, i.e., keep the standard structure unchanged. The most renowned scheme belonging to this category is the least square (LS) [11], which has been verified to be effective for indoor environments. However, for the vehicular environments, the LS estimator is incapable of updating the extremely time-varying channels. To cope with this problem, a number of schemes have been investigated [12]–[23]. In [12], a well designed Wiener filter was implemented to minimize the mean square error (MSE). In order to ensure satisfactory performance, the Wiener filter requires the knowledge of some prior information of the channel, which is difficult to obtain in practice. In [13], an iterative channel estimator was introduced by using general-

Part of this work has been accepted for publication in the IEEE Transactions on Intelligent Transportation Systems.

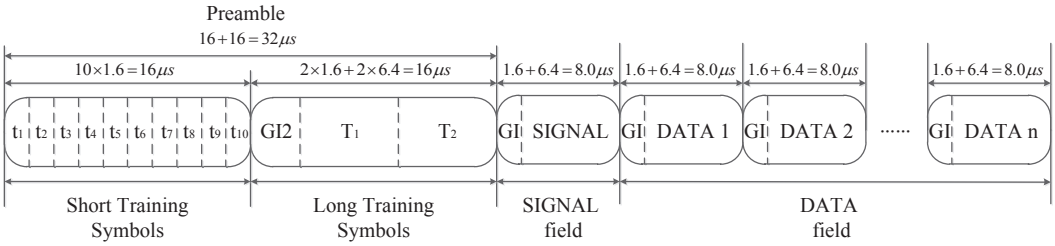

Fig. 1. IEEE 802.11p packet preamble structure.

ized discrete prolate spheroidal (DPS) sequences. Thereafter, the idea of DPS sequence was exploited in [14] and [15]. Although this approach follows the standard frame structure, it comes with high computational complexity. In [16] and [17], a technique named spectral temporal averaging (STA) was addressed. Therein, the CR is averaged in the frequency domain and the time domain successively to mitigate the dynamic nature of the vehicular channels. Nevertheless, the parameters in this scheme are determined empirically and vary for different channels. In [18] and [19], a decision-directed scheme was presented. However, in this scheme, decoding needs be implemented before channel estimation, which again results in high computational complexity. In [20]–[23], a theory was addressed by regarding data subcarriers as pilots, also referred to as pseudo-pilots. However, the performance enhancement of the pseudo-pilot scheme is very limited and the hardware design may be greatly challenging due to its increased complexity. Through comprehensive analysis, we observe that these existing schemes which belong to the second category exhibit some critical limitations. For example, most existing schemes require the receiver to have strong computational capability and some schemes rely on a priori channel statistics beforehand for estimating CRs. These limitations motivate us to design a new type of channel estimator. Our contributions in this report are summarized as follows.

1) Focusing on the limitations of existing channel estimation schemes, we propose a novel estimator named constructed data pilot (CDP), by exploiting the channel correlation characteristics of data symbols without any necessitation of a priori channel statistics.

2) We model the vehicular channel as a first-order Markov process. Thus, more accurate correlation values can be easily derived by means of the pilots inserted between data symbols, no matter which type of pilot pattern the standard follows.

3) By implementing minor modifications, the proposed estimators can be extended for most of the current orthogonal frequency division multiplexing (OFDM) based communication standards under vehicular time-variant channels.

The rest of this report is organized as follows. In Section II, we introduce the IEEE 802.11p standard and the channel model we use as system model. Section III gives a brief overview of two existing channel estimation schemes, namely LS and STA. The proposed CDP estimator along with its two modifications are elaborated in Section IV. Then, comparisons of bit error rate (BER) and frame error rate (FER) simulations, as well as computational complexity with the proposed estimators are presented in Section V. Finally, Section VI concludes this report.

II. System Model

A. Structure of the IEEE 802.11p

The IEEE 802.11p PHY is based on OFDM. Depending on different modulation and puncturing schemes, it can support data transmission rates ranging from 3 to 27 Mbit/s. The frame preamble structure of IEEE 802.11p is shown in Fig. 1. It has almost the same structure as that of IEEE 802.11a, except for the doubled symbol duration. Each frame consists of a preamble including short training symbols and long training symbols, a SIGNAL field, and a DATA field. The SIGNAL field conveys information about the type of modulation, the coding rate, etc., while the DATA field mainly comprises the transmitted data. The ten 1.6 μs short training symbols (t_1 to t_{10}) located at the beginning of every frame are used for coarse synchronization. The following two 6.4 μs long training symbols T_1 and T_2 are used for fine synchronization and channel estimation. The GI is inserted so as to mitigate inter-symbol interference. The SIGNAL field consists of only one OFDM symbol, while the number of symbols in DATA field is not explicitly defined.

For the IEEE 802.11p transmitter, a convolutional encoder is employed at the beginning for forward error correction. Higher data rate can be achieved by using puncturing, e.g., 2/3 and 3/4. The coded data is then interleaved so as to mitigate burst errors caused by impulse noises. Afterward, a modulation such as BPSK, QPSK, 16 quadrature amplitude modulation (16QAM) or 64QAM is adopted. Then, a 64-point inverse fast fourier transform (IFFT) implements the OFDM modulation. The 64 OFDM subcarriers include 48 data subcarriers and 4 phase tracking pilot subcarriers. Among them, the phase tracking pilots are located on subcarriers -21, -7, 7, and 21, which are used for compensating the common phase rotation caused by the residual frequency offset. In addition, 11 virtual subcarriers as well as a direct current subcarrier are also added to fill 64-point IFFT. Finally, GI and preamble are inserted.

B. V2V Channel Model

In the recent years, V2V channels have been extensively investigated (see [24]–[29] and the references therein). In this report, we adopt the model proposed in [24] and [25], which

has been adopted as a kind of standard V2V channel model dedicated for IEEE 802.11p. The measurement campaign was carried out in the metropolitan Atlanta, Georgia area including six scenarios, i.e., V2V Expressway Oncoming, V2V Urban Canyon Oncoming, roadside-to-vehicle (R2V) Suburban Street, R2V Expressway, V2V Expressway Same Direction with Wall, and R2V Urban Canyon.

Due to the space limit, we cannot give the results under all six vehicular scenarios. Simulations in this report are derived from two representative scenarios, i.e., V2V Expressway Oncoming and R2V Suburban Street. These two scenarios have covered typical vehicular environments including different communication types (V2V/R2V), different speeds (low velocity/high velocity), and a wide range of Doppler shift (400 –1200Hz).

III. Related Work

For comparison purposes, we present the two most representative channel estimation schemes for mobile communication standards in this section, namely LS and STA.

A. LS Estimator

The most commonly used channel estimation scheme for OFDM based communication standards is the LS estimator, which jointly utilizes the received preamble symbols. In general, a number of the current standards have two or more identical preamble symbols, e.g., $X(k)$. Take two preamble symbols as an example. We define the received symbols to be $R_{T_1}(k)$ and $R_{T_2}(k)$, hence, the CR is estimated as

$$H(k) = \frac{R_{T_1}(k) + R_{T_2}(k)}{2X(k)}. \tag{1}$$

In the same way, if the preamble comprises more than two symbols, Eq. (1) should be slightly modified. After Eq. (1), the estimated CR is used for equalization of the following data symbols assuming that the channel is static. However, LS estimator was proposed for relatively stationary environments such as indoor scenarios. When employed for vehicular environments with high mobility, it is incapable of estimating the highly time-varying characteristics. Thus, LS estimator will significantly deteriorate the system performance in practical use.

B. STA Channel Estimation Scheme

To alleviate the detrimental impact imposed by V2V channels, a scheme called STA was proposed in [16] and [17]. In this work, STA was defined as an enhanced equalization scheme, but in fact, it is an approach to estimate the dynamic channels.

The first step of the STA scheme is LS estimator, as in Eq. (1). Subsequently, the STA scheme is implemented iteratively. The $(i-1)$ estimated CR $H_{STA,i-1}(k)$ is used to equalize the received data symbol $S_{R,i}(k)$, giving rise to

$$\hat{S}_{T,i}(k) = \frac{S_{R,i}(k)}{H_{STA,i-1}(k)}, \tag{2}$$

where i represents the number of the OFDM symbol. Note that, $H_{STA,0}(k)$ is derived from the initial LS estimator, that is $H(k)$ in Eq. (1). $\hat{S}_{T,i}(k)$ is then demapped to obtain $\hat{X}_i(k)$. Note that, the demapped symbol $\hat{X}_i(k)$ on the pilot subcarriers is endued with the frequency domain value predefined in the standard. The initial channel estimate, $H_i(k)$ is obtained as

$$H_i(k) = \frac{S_{R,i}(k)}{\hat{X}_i(k)}. \tag{3}$$

It was further considered in [17] that since $H_i(k)$ was derived directly from the data symbols which may be incorrectly demapped, averaging of the initial estimates in both frequency and time domains is needed to improve accuracy. The frequency domain averaging is implemented as

$$H_{update}(k) = \sum_{\lambda=-\beta}^{\lambda=\beta} \omega_\lambda H_i(k+\lambda), \tag{4}$$

where $2\beta + 1$ represents the number of subcarriers that are averaged and ω_λ is a set of weighting coefficients defined by $\omega_\lambda = 1/(2\beta+1)$. The time-domain averaging is completed as follows which also turns out to be the final channel estimate,

$$H_{STA,i}(k) = \left(1 - \frac{1}{\alpha}\right) H_{STA,i-1}(k) + \frac{1}{\alpha} H_{update}(k), \tag{5}$$

where α is an updating parameter related to Doppler spread. The parameters α and β depend on the different types of vehicular channels. To ensure accuracy, α and β should be determined from the knowledge of the radio environment, e.g., from global positioning system and map knowledge referred in [17]. However, it is difficult to obtain these sort of environment information in practice. Therefore, it was suggested in [17] that, for simplicity and convenience, fixed values were chosen with performance degradation at an acceptable level.

IV. Proposed Channel Estimators

Motivated by the aforementioned limitations of the current channel estimation schemes, we propose a new type of estimators in this report. Except for the satisfactory BER and FER performance, our estimators adhere to standard OFDM structure, independent of any a priori information with very low computational complexity. In this section, we elaborate the three estimators based on the concept of CDP.

A. CDP Channel Estimator

It is widely understood that data symbols can hardly provide sufficient channel information since the receiver has no knowledge of the transmitted data beforehand. Accordingly, most existing schemes facilitate channel estimation via preambles or pilots. However, the preambles ahead of data symbols cannot support robust channel updates, especially under vehicular environments. Moreover, the pilots between data symbols are insufficient to track the variation in rapidly time-varying channels for a number of the current standards. In the sequel, we present a new approach to derive reliable estimation of CRs under time-variant mobile channels by constructing data pilots. Briefly, the data symbols are constructed to form

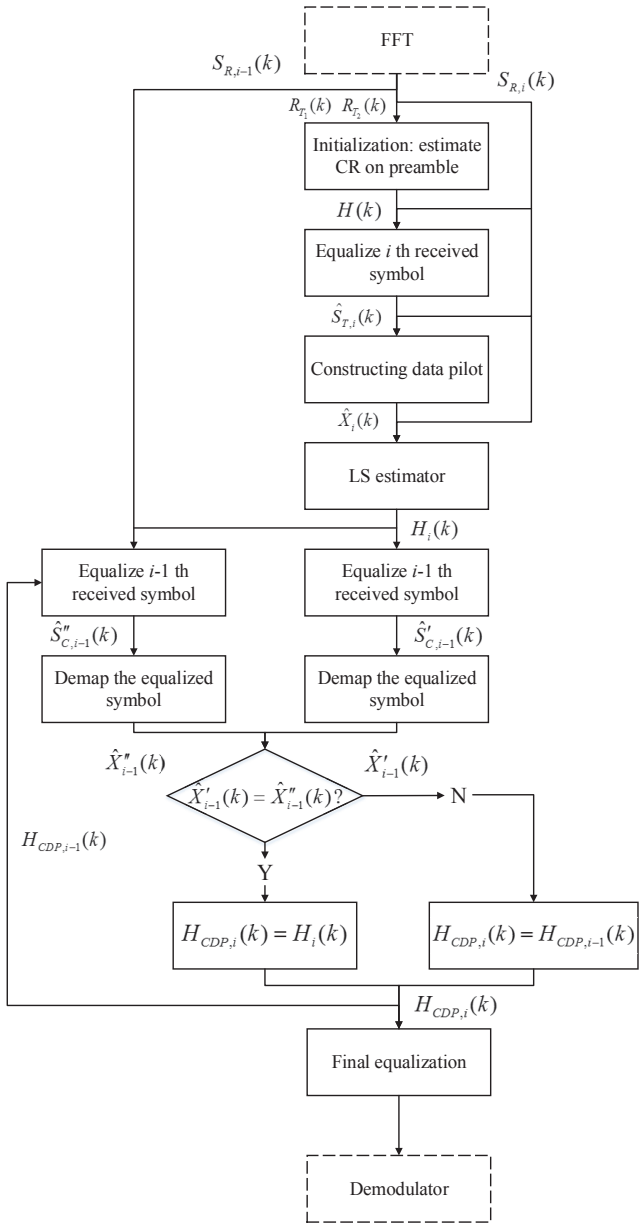

Fig. 2. Flow chart of the CDP estimator.

"pilots," under the assumption that the CRs associated with the neighboring symbols are highly correlated. Although these "pilots" are not accurate enough due to noise and interference, the inaccuracy can be mitigated through additional processing.

Fig. 2 depicts the flow chart of the CDP estimator. It is notable that the CDP estimator is implemented iteratively between fast Fourier transform (FFT) and demodulation operations, i.e., the two dashed boxes. Note that, $S_{R,i-1}(k)$, $S_{R,i}(k)$, $R_{T_1}(k)$, and $R_{T_2}(k)$ are the inputs of the CDP estimator, namely, the frequency-domain received symbols on the kth subcarrier, obtained from the FFT. It is worth noting that, k represents the index of data subcarriers, rather than those pilot subcarriers inserted between the data. As shown in Fig. 2, the CDP estimator is implemented iteratively. Specifically, the previous symbol's estimated CR, i.e., $H_{CDP,i-1}(k)$, which is the output of the CDP estimator, is employed to derive the following symbol's CR $H_{CDP,i}(k)$, which in turn serves as one of the inputs.

The CDP estimator comprises a preliminary step along with five main steps, including equalization, constructing data pilot, LS estimator, equalization & demapping, and comparison. With regard to the five main steps, the first three steps are similar to those in STA, while the last two take advantage of the correlation characteristics to improve the performance in the high SNR region, which is the notable difference between CDP and STA. These steps are detailed as follows.

Preliminary Step—LS estimator: In this step, LS estimator serves as the initial estimation by using Eq. (1). The estimated $H(k)$ is exploited to update the CR on the first symbol after the preamble, whose index number is $i = 1$. However, due to the difference in frame structure, the subsequent five steps are dedicated for those symbols $i > 1$, instead of $i = 1$. The specific procedure for estimating the first symbol's CR will be introduced after the elaboration of the following five steps.

Step 1—Equalization: As mentioned before, the CDP estimator iteratively updates the channel estimate by employing the previous symbol's CR since the CRs of the two adjacent data symbols are highly correlated. For ease of exposition, here, we assume that the CR of the current ith symbol is unchanged compared with its previous symbol's. Therefore, the first step – equalization is performed as

$$\hat{S}_{T,i}(k) = \frac{S_{R,i}(k)}{H_{CDP,i-1}(k)}, \tag{6}$$

where $H_{CDP,i-1}(k)$ is the output of the previous estimation process, i.e., $(i-1)$th symbol's estimated CR.

Step 2—Constructing Data Pilot: $\hat{S}_{T,i}(k)$ is then demapped to construct data pilots $\hat{X}_i(k)$, which is the core of the proposed scheme. Owing to the impacts of noise and other interferences, along with the inaccuracy of $\hat{S}_{T,i}(k)$ caused by our assumption, $\hat{S}_{T,i}(k)$ possibly falls into wrong quadrants. Therefore, $\hat{X}_i(k)$ is likely to be demapped to the incorrect constellation points, as shown in Fig. 3. By implementing demapping, the impact from noise and interferences can be partially alleviated. The remaining error will be further mitigated in the following steps by exploiting the correlation characteristics between channels within two adjacent symbols.

Step 3—LS Estimator: The constructed data pilot $\hat{X}_i(k)$ is subsequently utilized to calculate the ith data symbol's CR by using Eq. (3), i.e., the LS estimator. It should be noted that $H_i(k)$ is a relatively accurate estimated CR, though, it is not the final output of the CDP estimator.

Step 4—Equalization & Demapping: In the following two steps, the high channel correlation characteristics are exploited again to finally alleviate the impact from noise and interference brought from *Step 2*. $H_i(k)$ is first used to equalize $S_{R,i-1}(k)$ such that

$$\hat{S}'_{C,i-1}(k) = \frac{S_{R,i-1}(k)}{H_i(k)}. \tag{7}$$

Then, $S_{R,i-1}(k)$ is equalized by $H_{CDP,i-1}(k)$, i.e., the previous symbol's estimated CR, which has been used before in

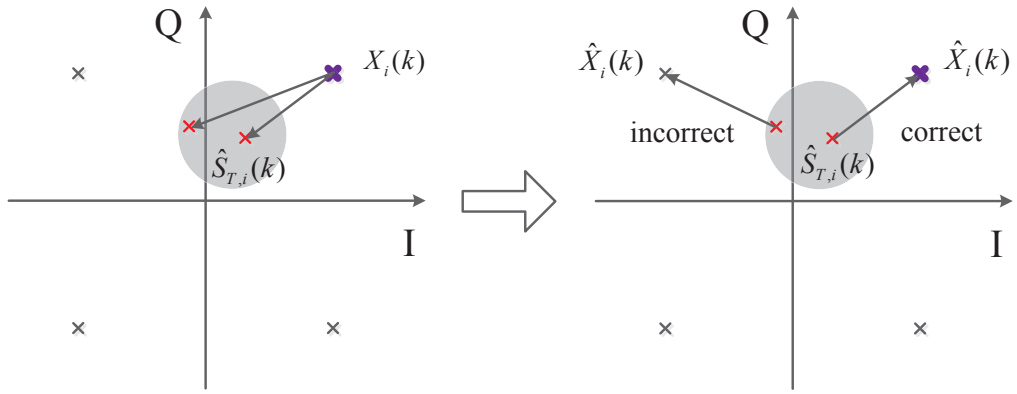

Fig. 3. Schematic diagram of constructing data pilot.

Eq. (6). The equalized $\hat{S}''_{C,i-1}(k)$ is given by

$$\hat{S}''_{C,i-1}(k) = \frac{S_{R,i-1}(k)}{H_{CDP,i-1}(k)}. \tag{8}$$

To compare $\hat{S}'_{C,i-1}(k)$ and $\hat{S}''_{C,i-1}(k)$, they are to be demapped to the corresponding constellation points $\hat{X}'_{i-1}(k)$ and $\hat{X}''_{i-1}(k)$.

Step 5—Comparison: As discussed before, the two adjacent data symbols have high correlation. Hence, if $\hat{X}'_{i-1}(k) \neq \hat{X}''_{i-1}(k)$, it indicates that the kth subcarrier's $\hat{X}_i(k)$, which is demapped after Eq. (6), is incorrect and we confirm that $H_{CDP,i}(k) = H_{CDP,i-1}(k)$, i.e., the previous symbol's estimated CR. Otherwise, if $\hat{X}'_{i-1}(k) = \hat{X}''_{i-1}(k)$, we have $H_{CDP,i}(k) = H_i(k)$.

In the *Preliminary Step*, we have briefly stated that the above five steps are proposed for the symbols whose index numbers satisfy $i > 1$ rather than $i = 1$. This is due to the fact that for the IEEE 802.11p, the preamble symbols are binary phase shift keying (BPSK) modulated to either 1 or -1. Hence, Eq. (7) cannot be employed directly. In addition, to ensure accuracy, the CR derived from LS estimator cannot be defined as $H_{CDP,1}(k)$. For these considerations, Eq. (7) should be modified as

$$\hat{S}'_{C,0}(k) = \text{real}\left(\frac{R_{T_2}(k)}{H(k)}\right), \tag{9}$$

where $R_{T_2}(k)$ is the last preamble symbol ahead of data symbols which are derived after FFT. From the property of the modulation scheme, if $\hat{S}'_{C,0}(k) > 0$, we have $\hat{X}'_0(k) = 1$, otherwise $\hat{X}'_0(k) = -1$. Note that, $\hat{X}''_0(k)$ is the known frequency-domain transmitted signal, i.e., $X(k)$. Afterwards, $\hat{X}'_0(k)$ and $\hat{X}''_0(k)$ are compared to determine $H_{CDP,1}(k)$. If $\hat{X}'_0(k) = \hat{X}''_0(k)$, we have $H_{CDP,1}(k) = H_1(k)$; otherwise, we have $H_{CDP,1}(k) = H(k)$, where $H(k)$ is obtained from LS estimator.

B. Modified CDP (MCDP) Channel Estimator

As will be demonstrated in the simulations section, the advantages of the CDP estimator can be summarized in three aspects: First and foremost, it can achieve excellent performance in comparison with STA, especially in the high SNR region. Second, the computational complexity of CDP is very low. Third, CDP estimator does not rely on any a priori channel statistics. However, the performance in the low SNR region is degraded and is even worse than STA. This is owing to the fact that in this case, the comparison procedure at low SNR is not accurate enough to track the dynamic nature of the time-variant channel. Attentive to this, we present a modification for the CDP estimator, named MCDP, by means of the first-order Markov process which can provide more accurate channel correlation.

1) First-Order Markov Process: As aforementioned, the CDP estimator is realized under the assumption that the correlation of the CRs between the two adjacent OFDM symbols is high. In essence, the high correlation characteristics are exploited twice in CDP, i.e., *Step 2* (constructing data pilot) and *Step 5* (comparison), respectively. It is evident that this assumption is quite beneficial for *Step 2* to construct data pilot, but seems rough for *Step 5*. Thus, it is necessary to derive the precise autocorrelation value one by one, so that the CR can be more accurately represented. According to [30], a time-variant channel can be modeled as a first-order Markov process using the so-called autoregressive model

$$H_m = \alpha H_{m-1} + \sqrt{1-\alpha^2} W_m, \tag{10}$$

where H_m denotes the mth symbol's CR and W_m is complex Gaussian variable following the distribution $\mathcal{CN}(0, \sigma_H^2)$. The kernel of this model is the autocorrelation coefficient α, which can be modeled as a zero-order Bessel function of first kind, i.e., $\alpha = J_0(2\pi f_d \tau)$, where f_d represents the maximum Doppler shift of the channel and τ is the time interval of the OFDM symbol.

The coefficient α can be easily derived via pilots, especially for comb-type pilots. Denote $H_{P,i}(k)$ as the CR on subcarrier k ($k \in \mathcal{N}_p$), in which $\mathcal{N}_p$ is the set of pilot subcarriers. Then,

we have

$$\alpha_{i,i+1} = \left| \frac{\sum\limits_{k\in\mathcal{N}_p} H_{P,i}(k)H^*_{P,i+1}(k)}{\sum\limits_{k\in\mathcal{N}_p} |H_{P,i}(k)|\,|H_{P,i+1}(k)|} \right|, \quad (11)$$

where $\alpha_{i,i+1}$ represents the autocorrelation of the CRs between the ith and $(i+1)$th data symbols. If an OFDM frame contains N data symbols, it means that the number of $\alpha_{i,i+1}$ that we finally obtain is $N-1$. For simplicity, the CR $H_{P,i}(k)$ can be derived from LS estimator since the pilots have been predefined in the frequency domain. By using Eq. (11), the autocorrelation of the CRs between the adjacent data symbols can be accurately and conveniently derived.

2) MCDP: By virtue of first-order Markov process, correlation characteristics can be more precisely exploited. Then, we will introduce the modification MCDP for CDP estimator based on the result of the first-order Markov process. In view of the limitation of CDP, we mainly focus on modifying the comparison procedure, namely *Step 5*. Inspired by Eq. (5) in [17], if $\hat{X}'_{i-1}(k) = \hat{X}''_{i-1}(k)$, we have

$$H_{CDP,i}(k) = (1-\frac{\alpha_{i-1,i}}{\rho})H_i(k) + \frac{\alpha_{i-1,i}}{\rho}H_{CDP,i-1}(k). \quad (12)$$

Conversely, if $\hat{X}'_{i-1}(k) \neq \hat{X}''_{i-1}(k)$, define that

$$H_{CDP,i}(k) = (1-\frac{\alpha_{i-1,i}}{\rho})H_{CDP,i-1}(k)+\frac{\alpha_{i-1,i}}{\rho}H_i(k). \quad (13)$$

Note that, ρ is a modifying coefficient related to the types of channels as well as modulation schemes. In addition, it is important to highlight that the condition for Eqs. (12) and (13) to hold is $i \geq 2$. When $i = 1$, we should follow the *Step 5* of CDP estimator. This is due to the fact that we cannot derive the autocorrelation α between the last preamble symbol and the first data symbol.

3) Optimal Value of ρ: Previously, we have mentioned that the value of ρ is related to BER performance under mobile channels. Table I reveals the relationship between the V2V channels, modulation schemes, and optimal values of ρ, in which velocities and Doppler shifts are drawn from [24] and [25]. Generally speaking, a higher Doppler shift or a higher order of modulation scheme implies a larger ρ. In practice, since the V2V channels are extremely dynamic, the optimal value of ρ varies from time to time during driving. As we know, the Doppler shift is related to the velocity for most cases. Hence, we can model ρ as a linear function with respect to velocity for different modulation schemes, in which the velocity can be measured by sensors on board. In addition, one can also alternatively set ρ as a constant for a given modulation scheme under all channel scenarios. For example, $\rho = 1.8$ for QPSK and $\rho = 2.0$ for 16QAM. Simulation results demonstrate that although the predefined constant may not be the optimal one, the difference of BER performance is minimal.

C. SNR-Assisted MCDP (SAMCDP) Channel Estimator

1) SAMCDP: As we discussed, modifications in Eqs. (12) and (13) are expected to be more suitable for a relatively low SNR. However, when SNR is sufficiently high, the BER performance of the conventional CDP estimator will outperform that of the MCDP. This is due to the fact that in high SNR region, the construction of data pilots, i.e., *Step 2* in the CDP estimator, is more accurate since the noise can be neglected. Therefore, the comparison in *Step 5* of CDP estimator is precise enough when SNR is high. On the contrary, Eqs. (12) and (13) bring about errors when the noise is minimal. Thus, for this case, it is better to choose CDP rather than MCDP. We will see that under all the mobile scenarios, the BER curves of CDP and MCDP have intersections, which correspond to approximately the same SNR. Therefore, in order to achieve optimal performance, we give a further modification to the MCDP estimator, named SAMCDP, by combining CDP and MCDP for different SNR regions. With regard to low SNR region, we prefer MCDP. When SNR is high enough, CDP is a better choice. To sum up, if $\hat{X}'_{i-1}(k) = \hat{X}''_{i-1}(k)$, we have

$$H_{CDP,i}(k) = \begin{cases} \left(1-\frac{\alpha_{i-1,i}}{\rho}\right)H_i(k) \\ +\frac{\alpha_{i-1,i}}{\rho}H_{CDP,i-1}(k),\ SNR \leq \gamma \\ H_i(k),\ SNR > \gamma \end{cases}, \quad (14)$$

otherwise, $H_{CDP,i}(k)$ becomes

$$H_{CDP,i}(k) = \begin{cases} \left(1-\frac{\alpha_{i-1,i}}{\rho}\right)H_{CDP,i-1}(k) \\ +\frac{\alpha_{i-1,i}}{\rho}H_i(k),\ SNR \leq \gamma \\ H_{CDP,i-1}(k),\ SNR > \gamma \end{cases}, \quad (15)$$

where γ is a predefined SNR threshold, which corresponds to the intersection of CDP and MCDP's BER (or FER) curves. Through simulations, we observe that no matter under which vehicular channel, γ is approximately 25dB. Detailed simulation results will be discussed in Section V. A.

2) SNR Estimation: In order to implement reliable SAMCDP estimator, the accuracy of estimated SNR is of great importance. However, it is difficult to derive the exact SNR for wireless channels, especially under mobile environments. A feasible way to realize SNR estimation was addressed in [31] by using the preamble ahead of data symbols, which was first proposed for the IEEE 802.16 standard. We notice that this SNR estimation approach is scalable for other OFDM based standards with similar preamble structure.

Specifically, SNR estimation is performed under the assumption that the CRs on the adjacent preamble symbols are invariant. For most standards, the preamble comprises two or more identical OFDM symbols, or one OFDM symbol with a number of identical parts. Therefore, the noise variance can be derived by averaging the square of the difference in the two received preamble symbols. Similarly, in view that the absolute value of preamble on each subcarrier equals to 1, the power of signal can be easily obtained.

Owing to the fact that the V2V channels we use for simulations in Section V were derived from road test, it is impossible to compare the practical MSE with the theoretical one. Nonetheless, we see that this SNR estimation approach has high accuracy. In particular, when the SNR is around $\gamma = 25$dB, the practical MSE can be reduced to 8%.

TABLE I
COMPARISON OF THE OPTIMAL ρ UNDER DIFFERENT CHANNEL MODELS AND DIFFERENT MODULATION SCHEMES

Scenario	Velocity (km/h)	Doppler Shift (Hz)	ρ (QPSK)	ρ (16QAM)
V2V Expressway Oncoming	104	1000–1200	2.1	2.4
R2V Urban Canyon	32–48	300	1.6	1.8
R2V Expressway	104	600–700	1.8	1.9
V2V Urban Canyon Oncoming	32–48	400–500	1.7	2.0
R2V Suburban Street	32–48	300–500	1.7	1.9
V2V Expressway Same Direction With Wall	104	900–1150	1.6	2.0

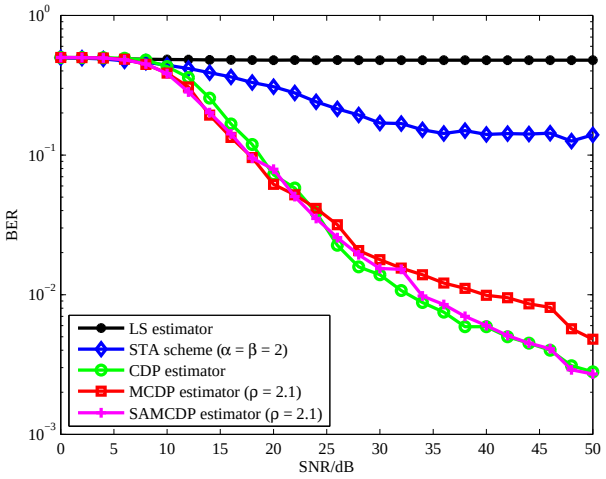

Fig. 4. Comparison of the BER performance of LS, STA, CDP, MCDP, and SAMCDP in QPSK modulation (V2V Expressway Oncoming).

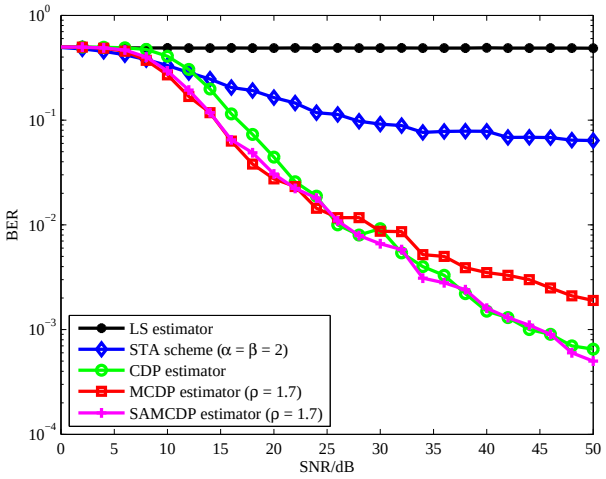

Fig. 5. Comparison of the BER performance of LS, STA, CDP, MCDP, and SAMCDP in QPSK modulation (R2V Suburban Street).

V. SIMULATIONS AND DISCUSSIONS

In this section, BER and FER simulations, as well as comparisons of computational complexity are conducted under IEEE 802.11p system. To examine the performances of our proposed CDP, MCDP, and SAMCDP estimators, LS and STA are taken as references.

A. BER and FER Performance

Figs. 4 and 5 depict the comparison results of the performance of LS, STA, CDP, MCDP, and SAMCDP in terms of BER with QPSK modulation under two V2V scenarios, including V2V Expressway Oncoming and R2V Suburban Street. Similarly, Figs. 6 and 7 show the FER performance with the same simulation setup. Due to the page limit, BPSK, 16QAM, and 64QAM modulation schemes are excluded. To achieve the optimal performance of the STA scheme, we set parameters $\alpha = \beta = 2$, as denoted in [17]. Similarly, when employing the MCDP and SAMCDP estimators, we let $\rho = 2.1$ for V2V Expressway Oncoming and $\rho = 1.7$ for R2V Suburban Street. Note that, the simulation configurations for both two scenarios are identical, no matter which kind of channel estimation schemes is chosen. Specifically, we use 800 frames for each simulation and 100 OFDM symbols for each frame.

First of all, we analyze the BER performance in accordance with Figs. 4 and 5. Clearly, the LS estimator remains at a relatively high level of BER for both scenarios. For the STA scheme, error floor emerges in the high SNR region. Therefore, we will not compare the BER performance of LS estimator and STA scheme hereafter. As discussed in Section III, the BER curves of CDP and MCDP intersect at about 25dB for both scenarios. By employing SNR estimation approach and defining a threshold of 25dB, the SAMCDP outperforms CDP and MCDP in both low and high SNR regions.

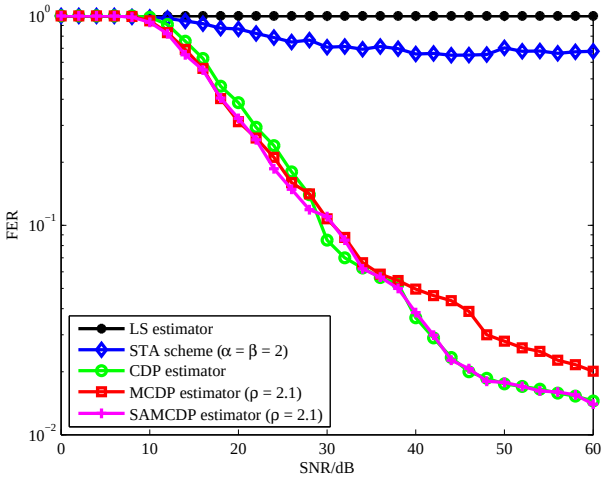

Fig. 6. Comparison of the FER performance of LS, STA, CDP, MCDP, and SAMCDP in QPSK modulation (V2V Expressway Oncoming).

We can also observe that since the V2V Expressway On-

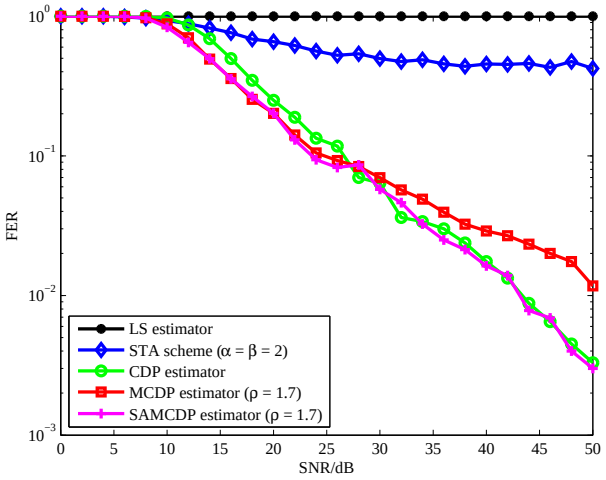

Fig. 7. Comparison of the FER performance of LS, STA, CDP, MCDP, and SAMCDP in QPSK modulation (R2V Suburban Street).

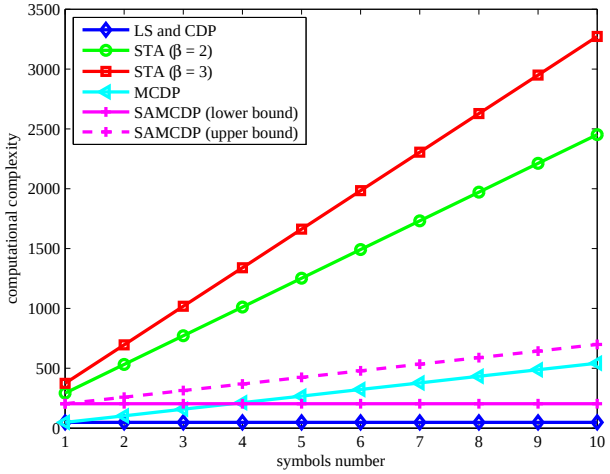

Fig. 8. Computational Complexity of Addition and Substraction.

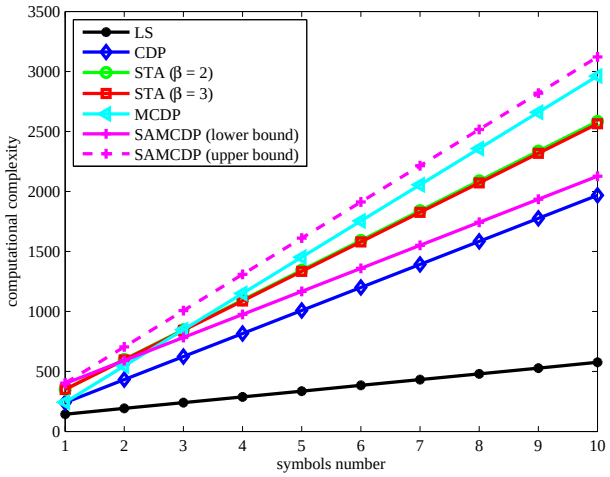

Fig. 9. Computational Complexity of Multiplication and Division.

coming channel has much higher Doppler shift, the overall performance has an obvious degradation with respect to that under R2V Suburban Street environment, which is shown in Fig. 5. In addition, since high mobility causes increased Doppler shift, the performance improvements of MCDP and SAMCDP in the low SNR region are impaired compared with that of CDP. According to Table I, we see that the velocities of the vehicles under V2V Expressway Oncoming scenario are more than 100km/h. Furthermore, the two vehicles were driving face to face, which yields double Doppler shift. Therefore, this scenario can be classified into the worst cases for V2V communications. Generally speaking, with regard to those scenarios which are better than V2V Expressway Oncoming, the improvements of MCDP and SAMCDP in the low SNR region are still significant.

Finally, we compare the FER performance shown in Figs. 6 and 7, which is critical for practical communication systems. In correspondence with the results of BER performance, the FER under V2V Expressway Oncoming has an obvious degradation compared with that under R2V Suburban Street scenario. Furthermore, the FER curves of CDP, MCDP, and SAMCDP estimators verify the foregoing analysis for BER performance. In other words, the SAMCDP estimator outperforms CDP and MCDP estimators in low and high SNR regions, respectively. We also see that all the three proposed estimators have satisfactory FER performance. For the simulated scenarios V2V Expressway Oncoming and R2V Suburban Street, the FER curves drop down to 10^{-1} at about 30dB and 25dB, which means that most frames can be received without error.

B. Computational Complexity

For the channel estimation schemes under vehicular environments, low computational complexity is indispensable for hardware design. In Section I, we have emphasized that a number of the current schemes must realize huge matrix multiplications, which results in immense computational complexity. Remarkably, they are incomparable with our proposed channel estimators. In this section, we only compare five most typical channel estimation schemes, i.e., LS, STA, CDP, MCDP, and SAMCDP, listed in Table II.

In Figs. 8 and 9, we present the comparison of the computational complexity for the five channel estimation schemes in accordance with Table II. Given that different arithmetical operations cost different amount of resources for hardware, we group the four operations into two types in the light of their respective properties, comprising addition and substraction, multiplication and division. In the sequel, we abbreviate these two types as addition and multiplication operations for simplicity.

Then, we will compare the computational complexity from the aspect of operations. It is evident that the complexities of LS in both addition and multiplication operations are minimal with respect to other four schemes, at the expense of a drastical performance degradation. For addition operation, as shown in Fig. 8, CDP has the lowest complexity, which is the same as

TABLE II
COMPARISON OF THE COMPUTATIONAL COMPLEXITY

Schemes	Addition	Substraction	Multiplication	Division
LS	48	—	—	$48N + 96$
STA	$52 + (2\beta + 1)(52 - 2\beta)N$	$48N$	$148N - 2\beta N$	$104N + 104$
CDP	48	—	—	$192N + 48$
MCDP	$56N$	$48N - 48$	$192N - 192$	$193N - 47$
SAMCDP	$99 \sim 56N + 51$	$53 \sim 48N + 5$	$104 \sim 192N - 88$	$192N + 51 \sim 193N - 44$

that of LS. This is because for both CDP and LS, addition operation only has to be implemented once, i.e., the LS estimator by exploiting the two long training symbols. Conversely, STA has the utmost complexity due to its averaging procedure. Furthermore, with the increase of β, the complexity of STA has an obvious leap. For MCDP and SAMCDP, we observe that SAMCDP's upper bound is higher than MCDP's due to the cost from SNR estimation. However, statistically, the overall addition operation of SAMCDP is less than MCDP. For multiplication operation, we infer that the average complexity of SAMCDP is similar with that of STA, both of which are much less than MCDP, but higher than CDP. According to the analysis above, we sort the total computational complexity as LS$<$CDP$<$SAMCDP$<$MCDP$\approx$STA.

In a nutshell, when taking BER and FER performance, as well as computational complexity into consideration, the proposed channel estimation estimators have obvious advantages. In particular, SAMCDP outperforms the other two estimators in BER and FER performance with relatively lower computational complexity.

VI. CONCLUSIONS

In this report, we focused on the channel estimation problem encountered in V2V environments for the IEEE 802.11p standard based systems. The issue is raised in view of the limitations of the current channel estimation schemes. First, the BER performance is unsatisfactory. Second, most existing schemes exhibit enormous computational complexity. Third, a number of the current schemes rely on a priori channel information. To overcome these deficiencies, we proposed a kind of channel estimators based on the concept of CDP, which can be utilized for most current communication systems without any a priori information. Simulations demonstrate that prominent performance can be achieved by employing CDP estimator, especially in the high SNR region. In addition, we accomplished two modifications for CDP. The first modification named MCDP, which models the V2V channel as a first-order Markov process. By doing so, more accurate correlation value can be easily derived through the pilots between data symbols and the BER performance in the low SNR region is improved. On the basis of CDP and MCDP, we presented a further modification called SAMCDP by utilizing a novel SNR estimation approach. Accordingly, for different SNR regions, CDP or MCDP estimators can be applied to ensure excellent performance in both low and high SNR regions. Simulations also reveal that the proposed channel estimators have lower computational complexity than the current ones.

REFERENCES

[1] H. Hartenstein and K. P. Laberteaux, "A Tutorial Survey on Vehicular Ad Hoc Networks," *IEEE Commun. Mag.*, vol. 46, no. 6, pp. 164–171, Jun. 2008.

[2] *802.11p-2010 IEEE Standard for Information Technology—Telecommunications and Information Exchange Between Systems—Local and Metropolitan Area Networks—Specific Requirements Part 11*, Wireless LAN Medium Access Control (MAC) and Physical Layer (PHY) Spec, 2010.

[3] C. F. Mecklenbräuker, A. F. Molisch, J. Karedal, F. Tufvesson, A. Paier, L. Bernad, T. Zemen, O. Klemp, and N. Czink, "Vehicular Channel Characterization and its Implications for Wireless System Design and Performance," *Proc. of the IEEE*, vol. 99, no. 7, pp. 1189–1212, Jul. 2011.

[4] R. Grünheid, H. Rohling, J. Ran, E. Bolinth, and R. Kern, "Robust Channel Estimation in Wireless LANs for Mobile Environments," *Proc. VTC-fall 2002*, pp. 1545–1549, Vancouver, Canada, Sep. 2002.

[5] S. I. Kim, H. S. Oh, and H. K. Choi, "Mid-amble Aided OFDM Performance Analysis in High Mobility Vehicular Channel," *Proc. IV'08*, pp. 751–754, Eindhoven, Netherlands, Jun. 2008.

[6] W. Cho, S. I. Kim, H. K. Choi, H. S. Oh, and D. Y. Kwak, "Performance Evaluation of V2V/V2I Communications: The Effect of Midamble Insertion," *Proc. Wireless VITAE'09*, pp. 793–797, Chennai, India, May 2009.

[7] J. Lin, "Channel Estimation Assisted by Postfixed Pseudo-Noise Sequences Padded with Null Samples for Mobile OFDM Communications," *Proc. IEEE WCNC 2008*, Las Vegas, USA, pp. 846–851, Mar. 2008.

[8] J. Lin, "Least-Squares Channel Estimation for Mobile OFDM Communication on Time-Varying Frequency-Selective Fading Channels," *IEEE Trans. on Veh. Tech.*, vol. 57, no. 6, pp. 3538–3550, Nov. 2008.

[9] J. Lin and C. Lin, "LS Channel Estimation Assisted from Chirp Sequences in OFDM Communications," *Proc. Wireless VITAE'09*, pp. 222–226, Chennai, India, May 2009.

[10] M. Muck, M. de Courville, M. Debbah, and P. Duhamel, "A Pseudo Random Postfix OFDM Modulator and Inherent Channel Estimation Techniques," *Proc. IEEE GlOBECOM 2003*, San Francisco, USA, pp. 2380–2384, Dec. 2003.

[11] M. K. Ozdemir and H. Arslan, "Channel Estimation for Wireless OFDM Systems," *IEEE Commun. Surveys & Tutorials*, vol. 9, no. 2, pp. 18–48, Jul. 2007.

[12] J. Nuckelt, M. Schack, and T. Kürner, "Performance Evaluation of Wiener Filter Designs for Channel Estimation in Vehicular Environments," *Proc. VTC 2011-Fall*, pp. 1–5, San Francisco, USA, Sep. 2011.

[13] T. Zemen and C. F. Mecklenbräuker, "Time-Variant Channel Estimation Using Discrete Prolate Spheroidal Sequences," *IEEE Trans. on Signal Process.*, vol. 53, no. 9, pp. 3597–3607, Sep. 2005.

[14] S. He and J. K. Tugnait, "On Doubly Selective Channel Estimation Using Superimposed Training and Discrete Prolate Spheroidal Sequences," *IEEE Trans. on Signal Process.*, vol. 56, no. 7, pp. 3214–3228, Jul. 2008.

[15] T. Zemen, L. Bernad, N. Czink, and A. F. Molisch, "Iterative Time-Variant Channel Estimation for 802.11p Using Generalized Discrete Prolate Spheroidal Sequences," *IEEE Trans. on Veh. Tech.*, vol. 61, no. 3, pp. 1222–1233, Mar. 2012.

[16] J. A. Fernandez, D. D. Stancil, and F. Bai, "Dynamic Channel Equalization for IEEE 802.11p Waveforms in the Vehicle-to-Vehicle Channel," *Proc. 48th Annual Allerton Conference*, pp. 542–551, Allerton, USA, Oct. 2010.

[17] J. A. Fernandez, K. Borries, L. Cheng, B. V. K. Vijaya Kumar, D. D. Stancil, and F. Bai, "Performance of the 802.11p Physical Layer in Vehicle-to-Vehicle Environments," *IEEE Trans. on Veh. Tech.*, vol. 61, no. 1, pp. 3–14, Jan. 2012.

[18] J. Ran, R. Grünheid, H. Rohling, E. Bolinth, and R. Kern, "Decision-Directed Channel Estimation Method for OFDM Systems with High

Velocities," *Proc. VTC-Spring 2003*, pp. 2358–2361, Jeju, Korea, Apr. 2003.

[19] T. Kella, "Decision-Directed Channel Estimation for Supporting Higher Terminal Velocities in OFDM Based WLANs," *Proc. GLOBECOM 2003*, pp. 1306–1310, San Francisco, USA, Dec. 2003.

[20] M. Chang and Y. Su, "Model-Based Channel Estimation for OFDM Signals in Rayleigh Fading," *IEEE Trans. on Commun.*, vol. 50, no. 4, pp. 540–544, Apr. 2002.

[21] M. Chang, "A New Derivation of Least-Squares-Fitting Principle for OFDM Channel Estimation," *IEEE Trans. on Wireless Commun.*, vol. 5, no. 4, pp. 726–731, Apr. 2006.

[22] M. Chang and T. Hsieh, "Detection of OFDM Signals in Fast Fading with Low-Density Pilot Symbols," *Proc. IEEE WCNC 2007*, pp. 1422–1427, Hong Kong, China, Mar. 2007.

[23] M. Chang and T. Hsieh, "Detection of OFDM Signals in Fast-Varying Channels With Low-Density Pilot Symbols," *IEEE Trans. on Veh. Tech.*, vol. 57, no. 2, pp. 859–872, Mar. 2008.

[24] G. Acosta-Marum and M. A. Ingram, "Six Time-and Frequency-Selective Empirical Channel Models for Vehicular Wireless LANs," *IEEE Veh. Tech. Mag.*, vol. 2, no. 4, pp. 4–11, Dec. 2007.

[25] G. Acosta-Marum, "Measurement, Modeling, and OFDM Synchronization for the Wideband Mobile-to-Mobile Channel," *Ph.D. dissertation*, Georgia Institute of Technology, Atlanta, GA, USA, 2007.

[26] I. Sen and D. W. Matolak, "Vehicle-Vehicle Channel Models for the 5-GHz Band," *IEEE Trans. on Intell. Transp. Syst.*, vol. 9, no. 2, pp. 235–245, Jun. 2008.

[27] J. Karedal, F. Tufvesson, N. Czink, A. Paier, C. Dumard, T. Zemen, C. F. Mecklenbräuker, and A. F. Molisch, "A Geometry-Based Stochastic MIMO Model for Vehicle-to-Vehicle Communications," *IEEE Trans. on Wireless Commun.*, vol. 8, no. 7, pp. 3646–3657, Jul. 2009.

[28] X. Cheng, C. -X. Wang, D. I. Laurenson, S. Salous, and A. V. Vasilakos, "An Adaptive Geometry-Based Stochastic Model for Non-Isotropic MIMO Mobile-to-Mobile Channels," *IEEE Trans. on Wireless Comm.*, vol. 8, no. 9, pp. 4824–4835, Sep. 2009.

[29] L. Bernadó, T. Zemen, F. Tufvesson, A. Molisch, and C. Mecklenbr äuker, "Delay and Doppler Spreads of Non-Stationary Vehicular Channels for Safety Relevant Scenarios," *IEEE Trans. on Veh. Tech.*, vol. 63, no. 1, pp. 82–93, Jan. 2014.

[30] W. C. Jakes, *Microwave Mobile Communications*, New York: Wiley, 1974.

[31] G. Ren, H. Zhang, and Y. Chang, "SNR Estimation Algorithm Based on the Preamble for OFDM Systems in Frequency Selective Channels," *IEEE Trans. on Commun.*, vol. 57, no. 8, pp. 2230–2234, Aug. 2009.